Experimental Data of a directional Borehole Radar System for UXO detection

Ronald van Waard
Department of Electromagnetic Security
TNO-FEL
The Hague, The Netherlands

Stefan van der Baan
T&A Survey
Amsterdam, The Netherlands

Koen W.A. van Dongen
Department of Electrical and Electronic Engineering
National University of Ireland
Cork, Ireland

***Abstract* — Ground penetrating radar (GPR) is a well-known method for exploring the subsurface. Typically, the antenna system is located at the surface. This approach is not feasible if the target of interest is beyond the detection range of this surface equipment, for example because this target is located too far away or behind a highly conductive barrier. Directional borehole radar is an effective method in these cases. In this paper, we present experimental data of a directional borehole radar for UXO detection. We describe the operation and results of an impulse directional borehole radar that was developed for UXO detection. Both laboratory and field data are shown and the types of processing that we apply on them. We will also describe some differences and similarities with impulse surface radar.**

Keywords–GPR; directional borehole radar; UXO detection;

I. Introduction

UXO (UneXploded Ordnance) detection in soft soils is a typical example where the object of interest is beyond the detection range of surface radar equipment. In this case, we have an overlaying clay/peat formation covering a sand layer, in which UXOs are situated. To make detection possible, a bistatic borehole radar system with a directional radiation pattern (3D-BHR) has been developed. This system explores the lateral surroundings from within one single borehole in order to detect the UXOs. The design of the antennas is described by Van Dongen [1], [2].

Borehole radar is a well known detection method for underground structures/objects. Cross-hole measurements as well as omni-directional and directional systems [3] are used, not only for object detection but also for geological mapping. Some potential oilfield applications are pointed out by Chen and Oristaglio [4]. Following the same line of reasoning, the USGS (U.S. Geological Survey) have made a directional borehole radar system for monitoring fluid invasion: a basic step for oil reservoir monitoring. In our detection application, penetration depth is the most important design parameter. Arcone [5] has remarked the importance of high data acquisition rates to allow noise reduction by trace stacking. Therefore high demands are put on the hardware of these directional systems. The second important design parameter is positioning accuracy.

II. Design of the tool

The 3D-BHR consists of two parts. One part contains various positioning sensors (magnetometer, gyroscopes, pressure/depth sensors), a temperature sensor and an electromotor which rotates the second part, the rotor. The rotor consists solely of the transmitting antenna, receiving antenna and their electronics. The two antennas are mounted at a fixed distance from each other. The 3D-BHR tool contains two wheel-blocks to guide and center the tool within the borehole. The 3D-BHR is connected to a console at the surface by means of a cable, where all commands are given and data received, recorded and monitored.

The antennas are designed such that they have directional radiation pattern [1]. To this end, the system contains an eccentric reflector plate and an eccentric dipole. All the antenna elements are embedded in water. This is done for two reasons:

- To reduce the wavelength of the electromagnetic waves in the antenna system. This enhances the directionality of the radiation pattern.
- The 3D-BHR is often used in water-saturated volumes, what automatically results in the fact that the borehole is filled with water. We achieve optimal coupling by embedding the antenna elements in water.

The antennas emit a transient electromagnetic wavefield with a center frequency of 100 MHz and a bandwidth of about 50 MHz. The received scattered wavefield is bandpass filtered and sampled with 8 bit A/D converter at a sampling frequency of 600 MHz, which corresponds to a sampling time of 1.67 ns. This high speed sampling enables us to measure 100 traces per second with a stackfold of 8. In general, one rotation contains at least 128 traces and is measured in less than two seconds. In a typical setup, we measure a complete rotation every 20 cm in borehole direction, giving us roughly 1 MB of raw data per meter borehole length.

The 50 MHz bandwidth is too small to obtain a sharp pulse. Hardware capabilities at the time of manufacturing, primarily in A/D conversion of the measured signal, is the main reason for this small bandwidth.

III. FIELD OPERATION

Prior to the measurements, a 10 inch diameter borehole (23 cm inner diameter) is drilled and a nonmetal casing is mounted to prevent collapsing of the open borehole. The fact that the borehole is filled with water, gives us a number of additional advantages:

- The water provides good electric grounding.
- The water enables good cooling for the electronics.
- The water pressure is used to measure the depth of the tool.
- The water damps sudden movements of the tool.

An impression of the 3D-BHR deployment is given in Figure 1.

Typically, the whole cylindrical volume surrounding the borehole is measured at once (C-scan). This is done using a so-called continuous helix-measurement. First the 3D-BHR is lowered to its maximum depth. Then measuring starts and, while the tool is lifted, the antenna rotates. Consequently, the angle-depth positional vector describes a helix-pattern.

IV. DATA PROCESSING AND OBJECT DETECTION.

We choose our processing techniques such that the resulting data are obtained near real-time and that detection is accomplished most easily. In addition, the data has become suitable for additional computational expensive imaging or inversion techniques later on, which could characterize the object by its electromagnetic medium parameters.

Radar data are collected simultaneously with other data from various sensors. Angular and depth information is provided by the positioning sensors, while the scattered electromagnetic waves are measured by the antennas and digitized by the electronics down hole. All raw data are then collected asynchronously and processed by the computer at the surface. Below, we give a descriptive overview of the processing techniques that we apply on the data. Results of processing on real data will be given in the next section.

Figure 1 Field operation of the 3D-BHR and test object.

A. *Preprocessing*

- Fixed gain scaling
- Positional processing
- Merging radar and positional data
- Zero-time correction
- Phase correction

B. *Binning*

Binning is the process of transforming the positions of the data from the 2D helical path to a 3D structured grid, with axes depth, angle and sample position. A bin is a measurement position with unique depth and angle and contains one trace (A-scan). The number of bins in angle and depth direction is chosen in advance. In the binning process, we choose or compute a trace for every bin. The new trace in a certain bin may be for instance the trace in the original data that is closest to the position of the bin, or it may be the average of some traces that are close to the position of the bin (mixing).

After the data are put in the 3D grid, we view the data in 2D planes (B-scans). We define two sorts of 2D planes: common-depth scans that contain traces, which all have an equal depth and common-angle scans, which contain traces that all have an equal angle.

C. *Direct wave removal*

Two methods are used for the removal of the direct wave, i.e. trace subtraction and muting.

The trace used for subtraction is obtained in a number of ways, a mean trace over either all data, or over common depth or common angle that the trace is part of.

Muting can also be done in two ways. One method is muting in time domain. Another more advanced method is muting in frequency domain, which resembles k-f domain filtering in surface radar. In the latter approach, the DC-component of the angular or depth-spatial Fourier transform is removed. This method is based on the assumption that the direct wave is relatively constant in angular and depth direction.

D. *Object detection*

When we interpret the data, we often look at either common-depth scans or common-angle scans. In this way, we cannot view data for multiple depths and multiple angles. However, for an operator, this is still the final check and provides the most reliable means for object position estimation.

Hence, to semi-automate the detection process, we use some simple, robust and fast techniques, that mainly search the data for amplitude changes. One method is to calculate the reflectivity of a trace and plot this value as a function of depth and angle. This method is sensitive to all kinds of scaling but less sensitive to noise. Another way is to apply analysis of variance in angular or depth direction. This method is influenced by noise, but less sensitive to data-independent scaling e.g. geometric spreading compensation. Data-dependent scaling e.g. automatic gain control (AGC), is avoided except for plotting common-angle or common-depth scans.

V. LABORATORY DATA

During a test setup, the borehole radar is positioned in an indoor water basin. The metal bottle that is shown in Figure 1, serves as object and is positioned at 1 m radial distance from the radar and 2 m below water surface. The bottle has a diameter of 12 cm and a length of 40 cm. Data are shown in Figure 2. The only processing that has been applied is removal of the direct wave by subtracting the first trace from the data set. Typically, the object continuously appears and disappears in the radar gram as a result of the rotational movement of the radar. In addition, we see the characteristic hyperbola, which is the result of the decreasing and subsequently increasing distance between the radar and the object as the radar passes the object vertically. The signal that is seen from sample 24 to 34 is the remainder of the non-perfect removal of the direct wave.

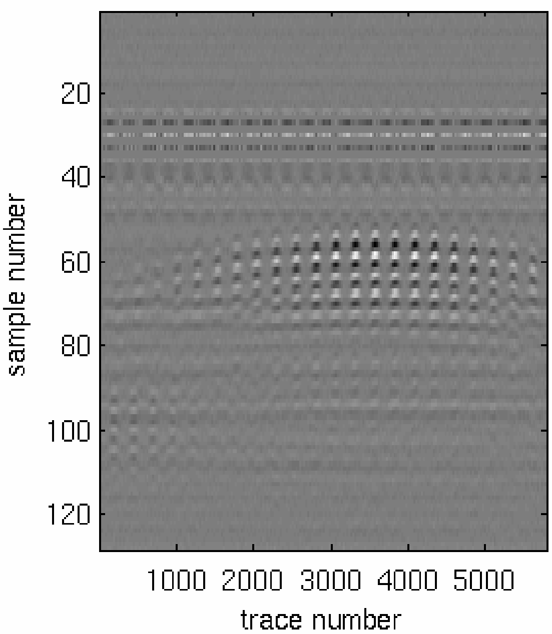

Figure 2 Laboratory data. The x-axis is the trace number, representing depth, since the radar moves from 4m to 1m depth while measuring traces. The number of traces per depth scan is 256.

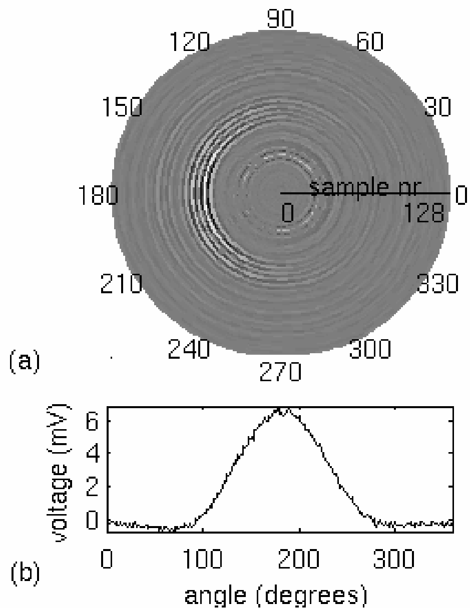

Figure 3 Angular view of the laboratory data shown in Figure 2. (a) One common-depth scan at depth of object which is located at 180 degrees in angular direction. (b) Sample 58 of this common-depth scan.

More detail of the measured signal in the angle direction is shown in Figure 3. In part (a), we see the data that are measured during one rotation at 2m depth (the depth of the object). The object is seen at 180 degrees in what we call a banana pattern. This pattern is the consequence of the choice of antenna design. The USGS system [6] has a similar pattern in angular direction. This pattern is explained easily, because the distance between radar and object is constant as the view point of the radar passes the object in angular direction. The measured data has the largest amplitude at the center of this banana (at 180 degrees) and decreases while moving away from this center. This is seen more clearly in part (b), where from this data the same (time) sample numbers are plotted.

VI. FIELD DATA

The field data are measured in a thick homogeneous sand body below the water table. A second borehole was drilled ten meters from the borehole radar in which the metal object of Figure 1 was positioned. The conditions (size and material of the object and the subsurface medium) are similar to the conditions in the detection of UXOs.

During data acquisition, preprocessing is done real time. After checking the raw data, a decision is made which method for direct wave removal is most appropriate. For this data, we subtracted the mean trace of the complete dataset and performed time domain muting afterwards. Next, we calculate the reflectivity, shown in Figure 4. A large reflectivity is observed at 6.4 m depth and at 350 degrees. Next, we show a common-depth scan at the depth of 6.5 m, see Figure 5, where an object appears at about 330 degrees. This corresponds to the actual position of the object! All the

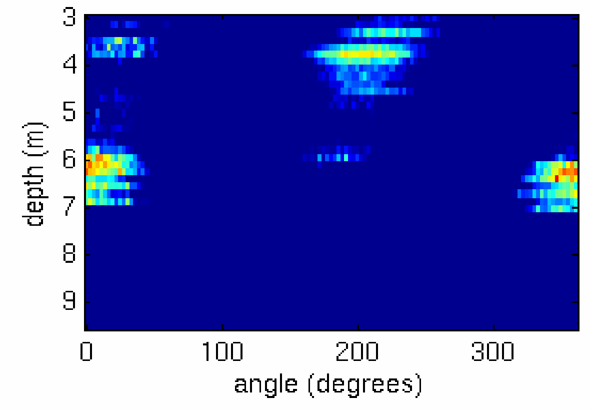

Figure 4 Reflectivity (90% clip) of field data over the whole data volume. Note that, an object is observed at 6.4 m depth and at 350 degrees. The accuracy can be improved by verifying B-scans.

other locations of interest that are shown in the reflectivity corresponded to other amplitude effects near the surface. Excavation of the whole volume a few months later, proved that there are indeed no other objects buried in this volume.

VII. Differences and Similarities with Surface Radar

We compare the borehole radar with bistatic (fixed offset) impulse-echo surface radars.

A major difference is the positioning of the probes of both systems in their hosting environments. In surface radar we have a two media problem, since the probe is positioned at the interface between two half-spaces: air and subsurface. For the borehole radar however, the probe is positioned in a

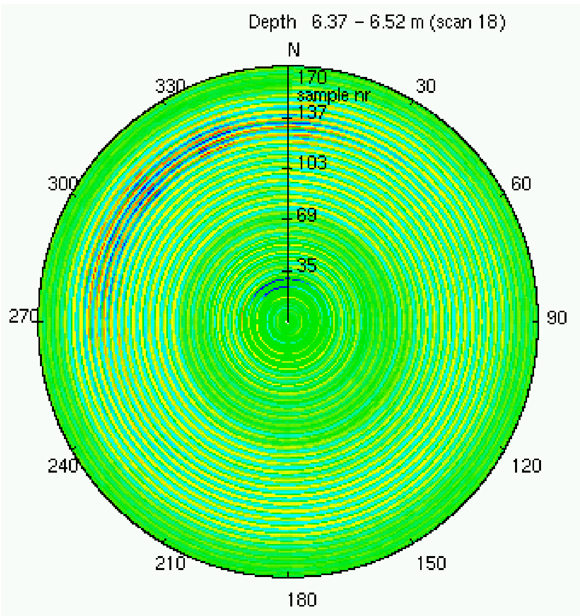

Figure 5 Field data, muted and mean depth scan subtracted. Shown is a depth scan at the depth of the object. The numbers around the scan denote the angle. The object is located at 330 degrees. Only the first 256 samples are shown.

cylindrical water column, which is surrounded by a medium saturated with water. Consequently, this can be approximated as a single medium problem. In addition the ambient noise level is lower because there are less electromagnetic sources within the subsurface

The data from the 3D-BHR needs similar static corrections to surface radar, when the borehole radar is not located in the middle of the borehole or when there are (water-filled) holes in between the borehole casing and its surrounding medium. Another similarity is the existence of two direct waves, one in the first medium (borehole) and one in the second medium (formation).

Similarities are that both GPR methods reveal hyperbolas in the data, while moving linearly over an object. For the borehole radar, in angular direction, there is no difference in travel time of the reflection. Therefore, we have no hyperbolas in this direction and the amplitude variation of the signal is not determined by changes in travel time.

Other differences are that, for directional borehole radar, the data throughput is much larger than for surface radar and that there is less amplitude resolution (8 bits). Finally, it is worth mentioning that deployment is a blind process.

VIII. Conclusions

The 3D-BHR is designed and tested for UXO detection in difficult situations, like at large depth, behind barriers and underneath existing constructions.

Obtained accuracy is typically 10 degrees in angular direction and 20 cm in depth direction. The resolution using 100 MHz antennas is large enough for detecting UXO-alike objects. Penetration depth is at least 10 m in homogenous sand bodies with low conductivity. Distance estimation is determined by the choice of the relative permittivity.

Differences of borehole radar with respect to surface radar have consequences for design and usage of the radar equipment and interpretation of its measured data.

References

[1] K.W.A. van Dongen, A directional borehole radar system for subsurface imaging, PhD thesis, Delft University of Technology, Laboratory of Electromagnetic Research, 2002.

[2] K.W.A. van Dongen, R. van Waard, S. van der Baan, P.M. van den Berg, and J.T. Fokkema, "A directional borehole radar system," Subsurface Sensing Techn. and Appl., An Int. Journ., vol. 3, Is. 4, pp. 327-346, October 2002.

[3] H.-T. Chang, Downhole pulse radar, U.S. Patent 4 814 768.

[4] Y.-H. Chen and M.L. Oristaglio, "A modeling study of borehole radar for oil-field applications", Geophysics, vol. 67, pp. 1486-1494, 2002.

[5] S.A. Arcone, "Field observations of electromagnetic pulse propagation in dielectric slabs", Geophysics, vol. 49, pp. 1763-1773, 1984.

[6] M. Peeters, J. Kovats, C. Moita, A. Pech, C. Moulton and J. Abraham, "Monitoring and modeling invasion using ground penetrating radar & flow simulation programs", 43rd annual symposium SPWLA, Oiso, Japan, June 3-5, 2002.